CNRS

Centre National de la Recherche Scientifique

INFN

Istituto Nazionale di Fisica Nucleare

Estimation of astigmatism losses in the Advanced Virgo non-degenerate recycling cavities

VIR-007A-09

Issue : 2

Date : July 24th , 2009

Massimo Granata, Matteo Barsuglia, Raffaele Flaminio

VIRGO * A joint CNRS-INFN Project
Via E. Amaldi, I-56021 – S. Stefano a Macerata - 56021 Cascina, Italia.
Secretariat: Telephone.(39) 050 752 521 * FAX.(39) 050 752 550 * e-mail virgo@virgo.infn.it

1. Introduction

In this document we present a study of the non-degenerate recycing cavities (NDRCs) for advanced Virgo, in terms of :

- losses induced by astigmatism
- tolerances to errors in the telescope parameters (radii of curvature and lenghts) and to thermal effects in the input test masses

Five different configurations for NDRCs have been studied : the four described in the note [1] by S. Hild, A. Freise and J. Marque and a new design (called 4bis), proposed by R. Flaminio, which should overcome some problems of the design #4.

The configuration 2, 3, 4 and 4bis use three curved mirrors : RM3 and RM2 for beam enlargement/reduction, and RM1 as power/signal recycling mirror (PRM/SRM). The configuration 2 and 3 have mirrors in different vacuum chambers but the same structure: RM2 and RM3 are in the common part of the interferometer. Configuration 4 and 4bis have the mirrors for enlargement/reduction (RM3, RM2) in each arm of the short Michelson.

Configuration n.1 is very similar to 2 and 3, but it uses additional converging lenses in the AR coating surface of the ITMs (or in the compensation plates, near the ITMs).

The study has been done using a Matlab based program, developed by the authors and described in the following. Where possible, a comparison with similar results obtained by AdLIGO have been done, and also a comparison of our code with independent *Finesse* simulations.

2. General design of NDRCs

The goal of the NDRC is to cumulate a Gouy phase inside the recycling cavity in order to separate the TEM_{00} from high order modes. For finesses of 40 and 70 (baseline for the adVirgo non-degenerate signal and power recycling cavity, respectively) the normalized build-up of the modes m+n=1 and m+n=2 is shown in the figure 1.

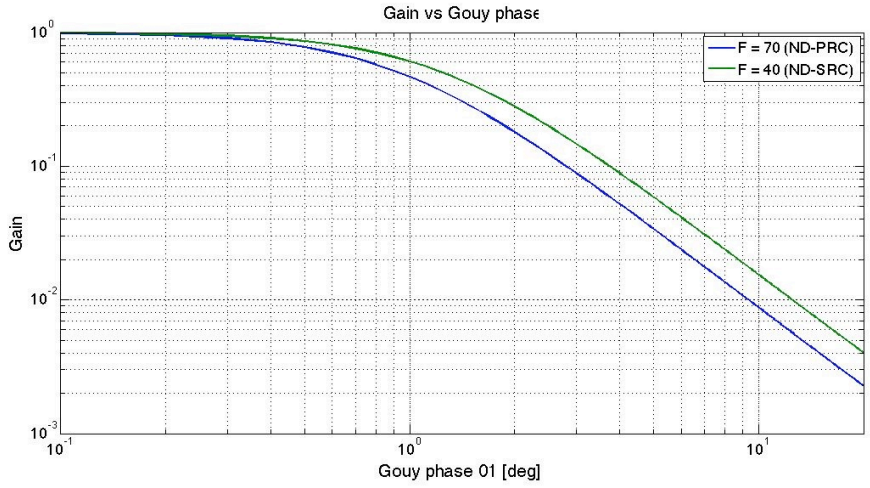

Figure 1 : normalized build-up vs Gouy phase. The accidental resonances have not been considered.

Given the limited space (few tens of meters) and the confocal parameter of the beam inside the arm cavities (few hundreds of meters), the beam coming from the arm cavities is in far field and its free propagation alone over few tens of meters gives a cumulated Gouy phase of a fraction of degree.

For this reason a folded configuration using 2 telescope curved mirrors and 1 recycling curved mirror has been proposed whithin the adLIGO community [2]. The same concept has been selected for adVirgo [3].

Guoy phase values of 160 deg and 20 deg have been initially proposed, following the adLIGO design.

For our simulations we have considered a Guoy phase of 20 deg. In principle, referring to fig.1, in order to ensure a good reduction of the high order modes even a smaller Gouy phase could be considered (i.e. a factor 100 of reduction for modes m+n = 2 is obtained with 4 degrees of Guoy phase).

3. Mismatching induced by astigmatism

Since the NDRCs are folded, the mirrors RM3 and RM2 are tilted and this induces astigmatism. The two planes, sagittal and tangential, are not coincident for the beam resonating in the NDRCs.

The power recycling cavity is coupled with the non-astigmatic input beam (output beam for the signal recycling cavity) and with the arm cavities, non astigmatic as well. Then for each recycling cavity there are two different sources of mismatch : the first one with the input beam (or output beam for the signal recycling cavity), and the second one with the arm cavities. Fig. A1 in Appendix A shows a scheme of the two different couplings.

The coupling between two gaussian beams can can be evaluated through the overlap integral γ, defined as the scalar product between the two normalized beams :

$$\gamma = < E_0(w1, R1) \mid E_0(w2, R2) >$$

with $E_0(w_i, R_i)$ being the TEM00 mode, and w_i and R_i being the beam radius and the beam front curvature respectively. For example, i = 1 is the arm cavity beam and i = 2 is the NDRC beam.

For an astigmatic beam, different beam parameters should be considered for the two transeverse directions : {w1x, R1x}, {w1y, R1y} for tangential and sagittal directions, respectively. The fundamental mode TEM_{00} can then be written as follows :

$$E_0 = \sqrt{\frac{2}{\pi}} \frac{1}{\sqrt{w_x w_y}} \exp\{-x^2(\frac{1}{w_x^2} + j\frac{k}{2R_x}) - y^2(\frac{1}{w_y^2} + j\frac{k}{2R_y})\}$$

then γ is equal to:

$$\gamma = \frac{2}{\pi}\sqrt{\frac{1}{w_{1x}w_{1y}w_{2x}w_{2y}}}\int_{-\infty}^{+\infty}\exp\left\{-x^2\left[\left(\frac{1}{w_{1x}^2}+\frac{1}{w_{2x}^2}\right)-i\frac{k}{2}\left(\frac{1}{R_{1x}}-\frac{1}{R_{2x}}\right)\right]\right\}dx$$

$$\cdot\int_{-\infty}^{+\infty}\exp\left\{-y^2\left[\left(\frac{1}{w_{1y}^2}+\frac{1}{w_{2y}^2}\right)-i\frac{k}{2}\left(\frac{1}{R_{1y}}-\frac{1}{R_{2y}}\right)\right]\right\}dy$$

4. Losses and mismatching

In order to make a correct design of the NDRCs, we have to compute how the mismatching induced by the astigmatism affects the interferometer sensitivity. In order to have a precise answer to this question, a simulation of the whole dual recycled interferometer (including at least the frequencial effects and the signal extraction scheme) is necessary.

In order to have a first assessment, we can compute the reduction of the power stored in the arms by the astigmatism inside the power recycling cavity. To do that, we need to know the relation between the mismatch (the overlap integral) and the reduction of the build-up in the cavities.

For a simple Fabry-Perot (FP) cavity illuminated by a slightly mismatched beam, the stored power P is a simple function of the overlap integral:

$$P/P_0 = \gamma^2$$

where P_0 is the stored power with perfect matching. We then define the *coupling losses* L as :

$$L=1-\gamma^2$$

In fig. 2 we show the comparison between the coupling losses (computed through the overlap integral) and the stored power computed with *Finesse* [4]. A cavity with the same finesse and geometry of the advanced Virgo arm cavity has been simulated. The cavity is illuminated with a beam whose waist is in the same position of the cavity waist, but whose size is slightly different from the cavity one.

If the mismatching is small and in the particular case of error in waist size only (the waist position is matched), we can also use the approximated analitycal formula by Anderson [5] :

$$L_{analit} = 1 - (w/w_0)^2$$

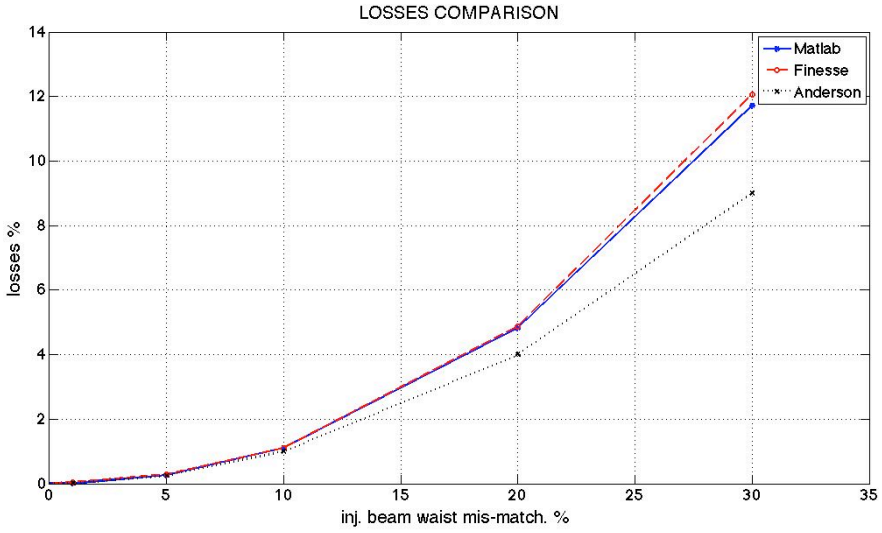

Figure 2 : Loss comparison plot for the single FP cavity scenario. Matlab refers to the computation of the coupling losses with the overlap integral.

As we see in fig.2, the power losses computed with *Finesse* are in good agreement with the coupling losses. The formula by Anderson start to diverge from 10% waist mismatch.

If we consider that the recycling cavity and the FP arm cavity are completely independent, we can compute the normalized build-up inside the power recycling cavity as : $P_{PRC}/P_0 = \gamma^2_{PRC}$, and the normalized build-up inside the FP arm cavity as : $P_{FP}/P_{PRC} = \gamma^2_{FP}$. The total decrease in the FP arm cavity build-up is then

$$P_{FP}/P_0 = \gamma^2_{PRC} * \gamma^2_{FP}$$

and the coupling losses can be written as follows :

$$L_{FP} = 1 - \gamma^2_{PRC} * \gamma^2_{FP}$$

In the real interferometer, the recycling cavity and the FP arm cavity are not decoupled, and the light which is not coupled into the FP cavity can still be recycled by the recycling cavity, then not being lost. In this sense the estimation of the losses can be considered as an upper limit. However, tests performed whithin the LIGO Collaboration [6] show that this assumption is valid with the advanced LIGO parameters, similar to the advanced Virgo ones. A preliminary comparison with *Finesse* simulations is discussed in appendix A, in order to test this result ; a detailed description of the simulations run under *Finesse* is also given in Appendix A.

5. Simulation code

The code that we developed is Matlab based, and performs the following computations :

1. Sagittal and tangential eigenmodes of the cavities.

The Fabry-Perot cavities are simulated through a set of ABCD matrices for both the tangential and sagittal planes [7] ; the optical parameters (lengths, radii of curvature, etc.) used in the elements of the matrices are those listed in [1]. The sagittal and tangential eigenmodes of NDRCs are found by solving the autoconsistency equation for a round trip of the beam in the cavity, with respect to q:

$$q = (Aq + B) / (Cq + D)$$

where q = z + i*zR is the complex gaussian parameter of the beam (z = distance to waist, zR = Rayleigh range).

2. Overlap integral and coupling losses.

The overlap integral and the coupling losses are computed using the formulas given in the previous paragraphs ; the overlap integral is calculated for the resonating beams of FP and NDRCs cavities in the steady state hypothesis, following the scheme of fig. A1 in Appendix A for the two different couplings. Only one arm of the interferometer is coupled to the NDRCs, in each simulation run (thus neglecting the short arm asymmetry).

3. Gouy phase.

The single trip cumulated Gouy phase is computed for the sagittal and tangential propagation.

4. Tolerances.

The different parameters of the design (ROCs and lengths) are varied automatically to find the tolerances in term of stability of NDRC and cumulated Gouy phase.

5. Checks.

The code has been tested imposing a null tilt angle for the recycling mirrors RM2 and RM3; in this case, the NDRCs are not affected by astigmatism and the mismatch losses are equal to zero.

Also the advanced LIGO NDRCs configuration [8] has been simulated, and the results for the astigmatism losses have been compared to those given by M. Arain in ref. [8] ; the losses computed with the code (1.68 %) are compatible with those simulated by Arain (1.5 %). We also find that the stability range of the recycling cavity is compatible to the one showed in ref. [2] (+/- 0.2% in the RM3 ROC).

6. Losses, Stability and Tolerances

In the following, a detailed description of loss estimation, stability and Gouy phase tolerances for every NDRC proposed design is given. For a brief description of these designs, and for the pictures and Optocad plots of their optical schemes, see [1].

For each of the NDRC design, the tolerances in terms of stability and Gouy phase are given.

Gouy phase tolerances are computed in order to obey the following condition : 10 > Gouy phase > 30 degrees.

For the computation of tolerances, each parameter is changed independently from the others.

For each NDRC design a summary table is given, as well as a colour plot (which we call *stability plot*) showing the coupling losses versus the percentage variation of the radius of curvature (ROC) of RM3 and RM2. In all plots, the regions of instability of the NDRCs are in white. For all the scenarios the plot is first given in a range of ROC variation of 1%, in order to appreciate the differences in the tolerances between different scenarios ; then a more detailed description of parameter tolerances is reported for each scenario, with dedicated stability plots.

All the simulations (except for scenario 1, which has a lens in each input test mass) have been run using an infinite ROC for the input test mass (ITM) antireflective (AR) surface ; all simulations refer to 20 deg Gouy phase scenarios.

6.1 Design n. 1 (lenses in the ITMs).

In this design there are three focusing elements: the lens in the AR coating of the ITMs and the two curved mirrors RM3 and RM2.

The presence of the lens before the beam-splitter (BS) introduces an asymmetry between the X and Y arms of the short Michelson, much higher than in others designs. For this reason, for this design we consider the X and Y arm separately.

6.1.1 Tolerances and losses.

For each arm of the short Michelson, the recycling cavity is stable for the optical parameters indicated in [1], but the recycling cavity formed with only the X arm and the one formed only with the Y arm have different losses and different stability plots (see fig.3 and 4). The working point of the interferometer is indicated in each plot by the (0 % , 0 %) point.

For the nominal values of the parameters [1] the coupling losses for the X and the Y arm differ of about a factor of 10 (0.26 % on X, 2.5 % on Y). In order to decrease the losses on the Y arm with respect to the ones of the X arm, so making the ITF more symmetric, we change the PRM3 ROC, so that the new set of optical parameters of the scenario is :

NDPRC design 1	
Space	rough distance [m]
IMx – BS (lx)	6.26
BS – PRM3 (lprm3)	10.7
PRM3 – PRM2 (lprm2)	4.5
PRM2 - PRM1 (lprm1)	4.5

	IMX AR side	BS	PRM3	PRM2	PRM1
ROC [m]	- 10.8000	Inf.	38.6810	- 2.1600	- 5.5900

The mirrors PRM3 and PRM2 are tilted of 2.5 and 3.5 deg respectively. The lenses are tilted by 1 degree, in order to avoid problems of back-scattered light. For this configuration the cumulated Gouy phase is Φ_G = 16.7 deg on the sagittal direction and Φ_G = 15.9 deg on the tangential direction for the X arm, and Φ_G = 24.3 deg on the sagittal direction and Φ_G = 28.7 deg on the tangential direction for the Y arm.

The astigmatism losses L_{FP} are :

X arm 1.1 % Y arm 1.3 %

Stability and sagittal Gouy phase tolerances for scenario n. 1 are listed in the following table :

	Stability tolerances %		Gouy phase tolerances % [10 deg < Φ_G < 30 (sagitt. plane)]	
lx	+ 2.45	- 0.24	+ 0.26	- 0.17
l3	+ 1.44	- 0.14	+ 0.16	- 0.10
l2	+ 1.78	- 0.17	+ 0.19	- 0.12
l1	+ 25.0	- 17.4	+ 12.35	- 11.25

ITM AR (lens)	+ 0.06	- 0.61	+ 0.04	- 0.07
PRM3	+ 0.48	- 4.9	+ 0.32	- 0.53
PRM2	+ 11.67	- 0.8	+ 1.0	- 0.6
PRM1	+ 100	- 14.0	+ 24.2	- 10.2

Since for this scenario there is a difference between the X and the Y arm, reported tolerances are chosen with this criterium : between the X and the Y values, the most strict tolerances - valid for both configurations - are reported. Tolerances listed in the table are asymmetric because the working point of the recycling cavity formed with the X arm only is near the upper border of the stability region.

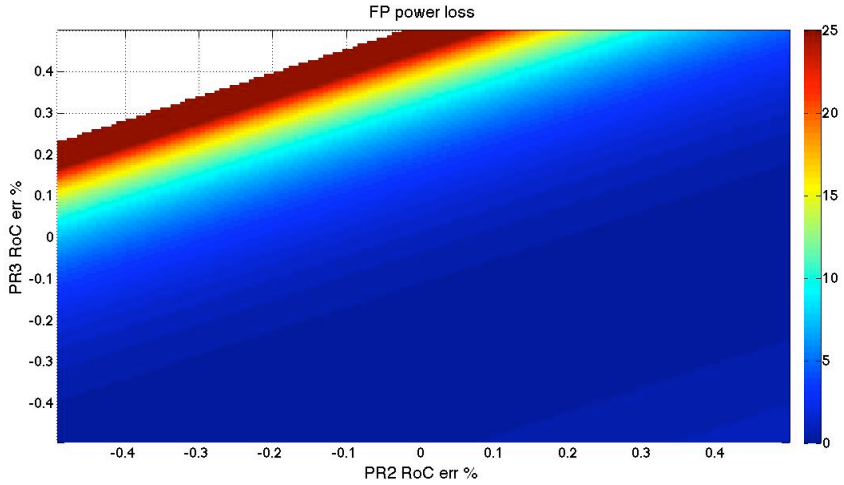

Figure 3: Stability plot, X arm – **design 1**

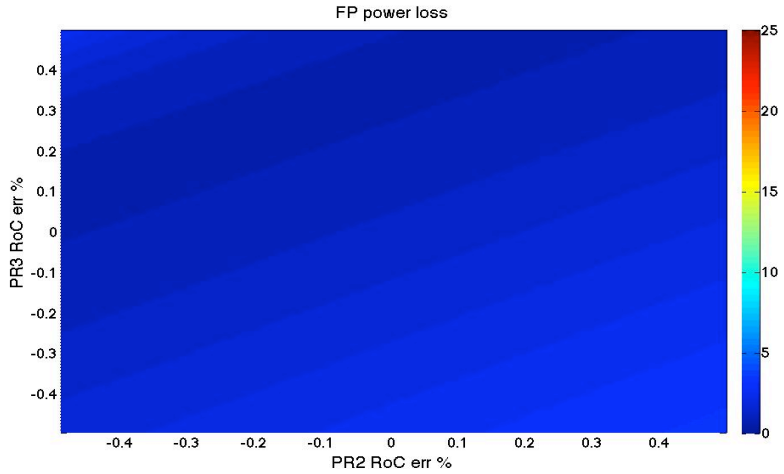

Figure 4: Stability plot, Y arm – **design 1**

6.1.2 Compensation of errors on ROCs.

Manufacturing errors in ROCs can be compensated changing the lengths of the telescope.

From the previous table we see that the most critical component of this design is the ROC of the lens. In fig.5, a stability plot of the lens ROC versus lx (length between the ITM and the BS) is reported: this plot is meant to shown how lx should change to recover the stability region (coloured region of the plot) for any given ITM AR ROC manufacturing error.

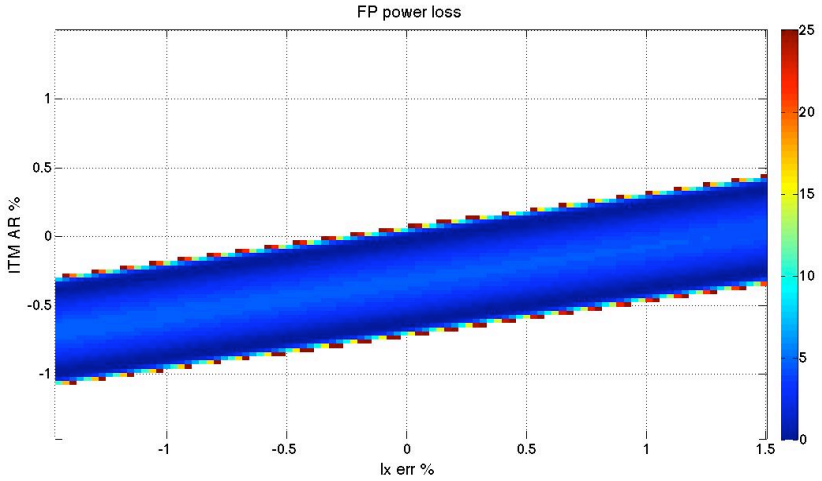

Figure 5 : Stability plot, ITM AR lens manufacturing error VS lx percentage variations – **design 1**

For example, if we have an error of + 0.1 % on ITM AR ROC (corresponding to about 1 cm), one should change lx length of at least + 0.5 % (corresponding to about 3 cm) in order to restore the stability of the NDRC ; variations of the same order would be required for lprm2 and lprm3, in order to recover an error of + 0.1 % on ITM AR ROC. Changing the length of lprm1 would have no effect at all (fig.6).

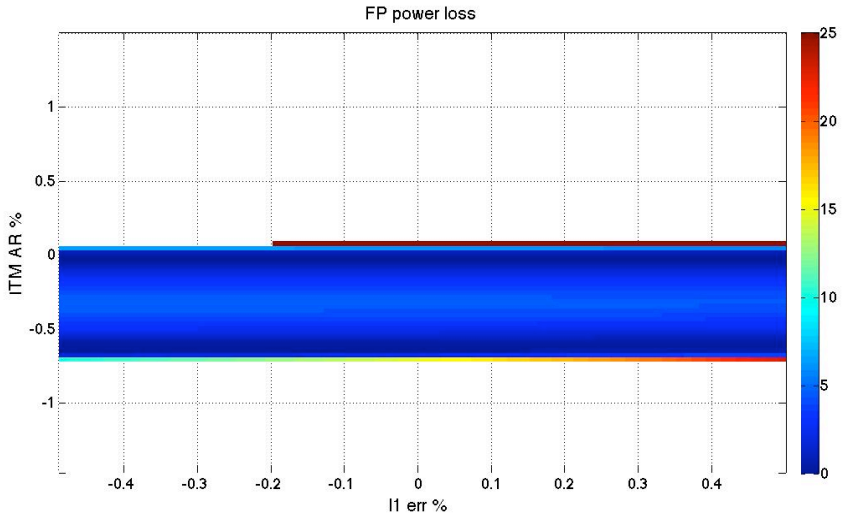

Figure 6 : Stability plot, ITM AR lens manufacturing error VS lprm1 percentage variations, **design 1**

The tolerances on PRM3 and PRM2 ROC manufacturing errors are less critical, but a similar argument applies also in this case: percentage variations of the same order of lx, lprm3, lprm2 would be required in order to recover ROC errors on the focusing elements, while changing lprm1 would have no effect on the stability of the NDRC.

6.2 Design n. 2 (advanced Virgo baseline design).

6.2.1 Tolerances and losses.

The tilt angle for PRM3 and PRM2 reported in [1] is 3.3 deg ; as a first attempt we tried to simulate the configuration with 160 deg of cumulated Gouy phase, but with this tilt angle the sagittal and tangential direction were not stable at the same time. Furthemore, according to the Optocad plots in [1] (made by J. Marque) the angle could be reduced to 1.7 deg, value for which the sagittal and tangential eigenmode are both stable. In the following we present the results of the simulation with for cumulated Gouy phase of 20 deg, where we kept the value of 1.7 deg for the tilt of PRM3 and PRM2.

The new set of parameters for this scenario is then the following :

NDPRC design 2	
Space	rough distance [m]
IMx – BS (lx)	5.5
BS – PRM3 (lprm3)	6
PRM3 – PRM2 (lprm2)	5.5
PRM2 - PRM1 (lprm1)	10.5

	IMX AR side	BS	PRM3	PRM2	PRM1
ROC [m]	Inf.	Inf.	12.7949	- 2.0418	- 2.0355

For this configuration the cumulated Gouy phase on the sagittal direction is Φ_G = 25.1 deg, and Φ_G = 47.57 deg on the tangential direction.
The astigmatism losses L_{FP} are:

X arm 6.8 % Y arm 6.8 %

The central part of the coloured region corresponds to a sagittal Gouy phase of 30 deg, instead of 20 deg, this is the reason because the working point (0 %, 0 %) of this design is closer to the upper border of the stability region (fig.7) ; for the same reason, the tolerances are asymmetric.

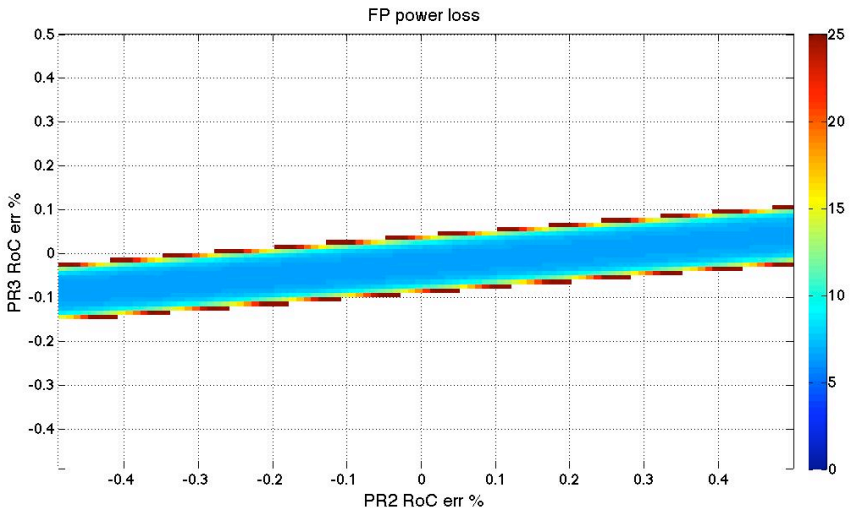

Figure 7 : Stability plot, **design 2**

Stability and sagittal Gouy phase tolerances for scenario n. 2 are listed in the following table :

	Stability tolerances %		Gouy tolerances % [10 deg < Φ_G < 30 (sagitt. plane)]	
lx	+ 100	- 100	+ 100	- 100
l3	+ 100	- 100	+ 100	- 100
l2	+ 0.112	- 0.044	+ 0.017	- 0.037
l1	+ 8.04	- 3.96	+ 1.48	- 3.28
PRM3	+ 0.03	- 0.09	+ 0.03	- 0.02
PRM2	+ 0.72	- 0.27	+ 0.12	- 0.24
PRM1	+ 100	- 20.5	+ 11.2	- 17.6

Since for this scenario there is no significant difference between the X and the Y arm, tolerances are valid for both configurations.

6.2.2 Compensation of errors on ROCs.

In fig.8, a stability plot of RM3 versus lprm2 is reported: this plot shows how much lprm2 (the distance between RM3 and RM2) should vary to recover the stability region for any given RM3 ROC manufacturing error.

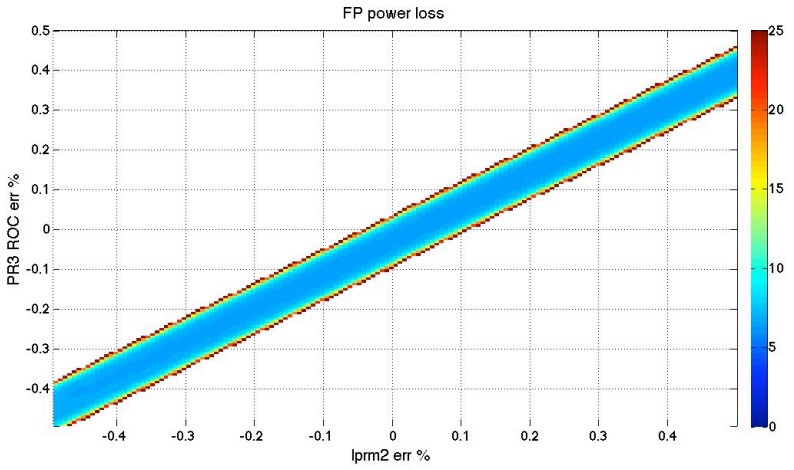

Figure 8 : Stability plot, PRM3 manufacturing error VS lprm2 percentage variations, **design 2**

Referring to fig.8, if the ROC of PRM3 has an error of + 0.1 % (corresponding to an error of about 1 cm), the length of lprm2 should be changed consequently of about + 0.1% (corresponding to about 5.5 mm) to recover the stability of the recycling cavity.

In general, the required percentage change of the distance lprm2 is equal to the percentage error in the PRM3 ROC.

In fig.9 the same plot for PRM2 vs lprm2 is reported :

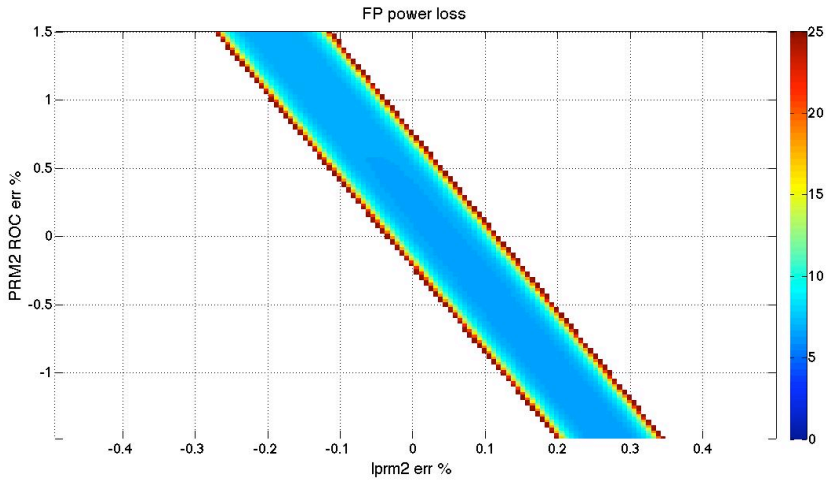

Figure 9 : Stability plot, PRM2 manufacturing error VS lprm2 percentage variations, **design 2**

Since between the ITM and PRM3 the recycling cavity eigenmode is in far field, small variations (of the order of 0.5 % , i.e. of the order of 3 cm) of lx or lprm3 have no consequences on its stability ; only a variation of lprm2 can recover manufacturing errors on PRM3 and PRM2.

Since the radio frequency sidebands must resonate in the NDRCs, a change of any cavity length should be compensated by an equal variation in some other length, to keep the overall cavity length unchanged. We checked the possibility of recovering the stability region by changing lprm2, and keeping constant the overall cavity length changing also lprm3. After all the length changes, we have checked that the Gouy phase value is the same whthin a few degrees.

Because of their general similar design, these considerations about compensation of ROC errors apply to all scenarios 2, 3, 4, 4-bis.

6.3 Design n. 3

6.3.1 Tolerances and losses.

The recycling cavity is unstable for the optical paramters given in [1], for a tilt of 1.9 deg of both PRM3 and PRM2. We change the ROC of PRM3 and PRM1, to obtain the sagittal matching of the FP and the NDRC ; since in this case the working point is near the border of the stability region, we slightly change PRM3 ROC to move towards the center of the region. The optical parameters of this scenario are then the following :

NDPRC design 3	
Space	rough distance [m]
IMx – BS (lx)	6.23

BS – PRM3 (lprm3)	6
PRM3 – PRM2 (lprm2)	12.05
PRM2 - PRM1 (lprm1)	16.87

	IMX AR side	BS	PRM3	PRM2	PRM1
ROC [m]	Inf.	Inf.	-27.5559	4.2300	6.6464

For this configuration the cumulated Gouy phase on the sagittal direction is Φ_G = 25.2 deg, Φ_G = 39.6 deg on the tangential direction, and astigmatism losses L_{FP} are:

X arm 3.7 % Y arm 3.7 %

In fig.10 the stability plot for this working point is reported.

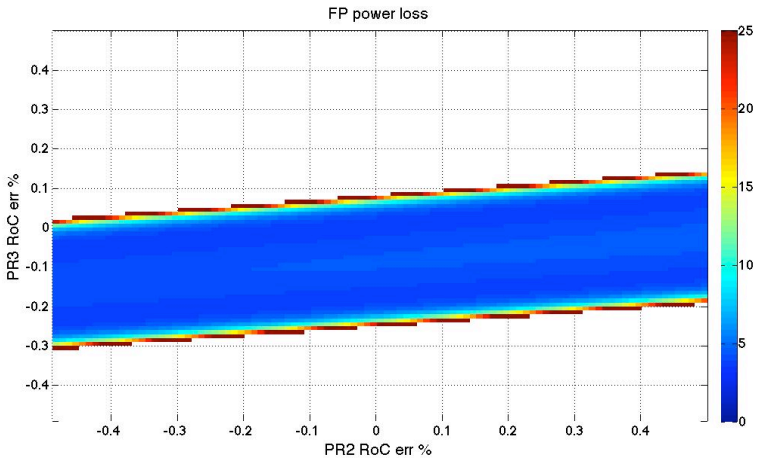

Figure 10 : Stability plot, **design n.3**

Tolerances for scenario 3 are reported in the following table :

	Stability tolerances %		Gouy tolerances % [10 deg < Φ_G < 30 (sagitt. plane)]	
lx	+ 100	- 100	+ 100	- 100
l3	+ 100	- 100	+ 100	- 100
l2	+ 0.3	- 0.09	+ 0.035	- 0.077
l1	+ 20.5	- 9.05	+ 3.1	- 7.45
PRM3	+ 0.07	- 0.25	+ 0.06	- 0.03
PRM2	+ 2.15	- 0.6	+ 0.25	- 0.5
PRM1	+ 100	- 23.0	+ 12.8	- 20.0

Since for this scenario there is no significant difference between the X and the Y arm, tolerances are valid for both configurations.

6.3.2 Compensation of errors on ROCs.

Figures 11 and 12 show the percentage variations of PRM2 and PRM3 (due for example to manufacturing errors) vs the length percentage variation of lprm 2; also for this scenario, as for scenario n.2, variations of the length of lprm2 are determinant to restore the stable working point of the NDRC.

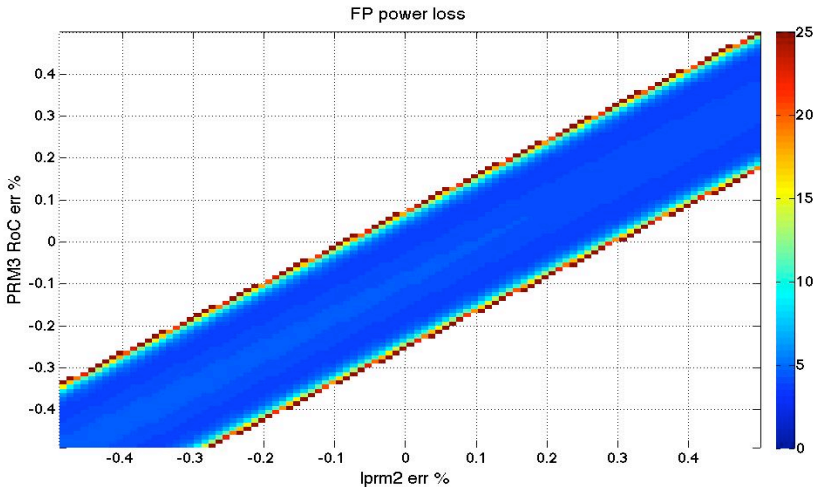

Figure 11 : Stability plot, PRM3 ROC error VS lprm2, **design n.3**

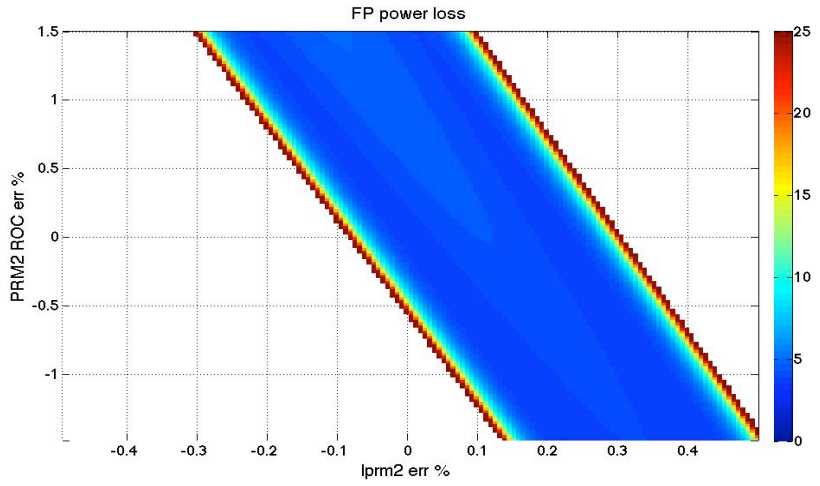

Figure 12 : Stability plot, PRM2 ROC error VS lprm2, **design n.3**

6.3 Design n. 4

6.4.1 Tolerances and losses.

For the optical paramters given in [1], with a tilt of 1.9 deg of both PRM3 and PRM2, the NDRC is unstable ; so we change the ROC of PRM3 and PRM1 to match the sagittal modes of the FP and the NDRC. The optical parameters of this working point are listed in the following table:

NDPRC design 4	
Space	rough distance [m]
IMx – PRM3 (lprm3)	12
PRM3 – PRM2 (lprm2)	12
PRM2 – BS (lx)	6.5
BS - PRM1 (lprm1)	10.5

	IMX AR side	BS	PRM3	PRM2	PRM1
ROC [m]	Inf.	Inf.	-27.9608	4.2300	4.6156

The cumulated Gouy phase on the sagittal direction is Φ_G = 23.6 deg, and Φ_G = 38.9 deg on the tangential direction for this working point ; astigmatism losses L_{FP} are :

X arm 3.3 % Y arm 3.3 %

The stability plot for this working point is reported in fig.13.

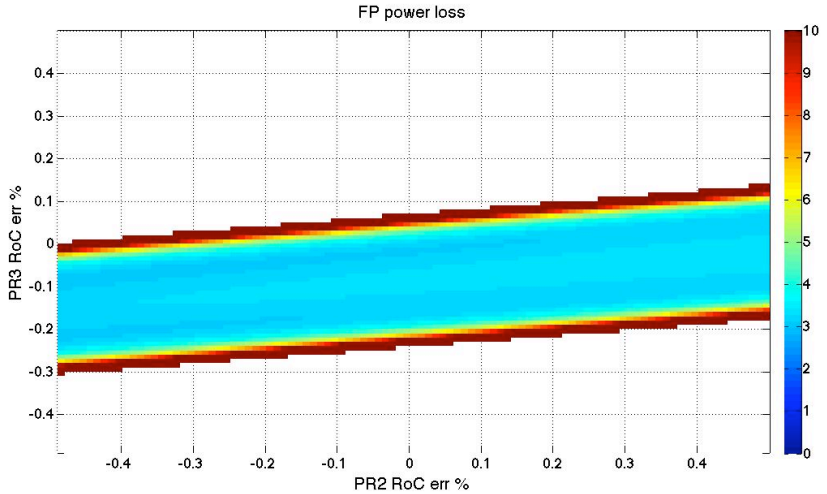

Figure 13 : Stability plot for **design 4**

Tolerances for design 4 are :

	Stability tolerances %		Gouy tolerances % [10 deg < Φ_G < 30 (sagitt. plane)]	
lx	+ 39.0	- 13.4	+ 7.0	- 10.8
l3	+ 100	- 100	+ 100	- 100
l2	+ 0.3	- 0.077	+ 0.046	- 0.062
l1	+ 24.7	- 8.2	+ 4.6	- 6.6
PRM3	+ 0.06	- 0.25	+ 0.05	- 0.04
PRM2	+ 1.9	- 0.45	+ 0.28	- 0.38
PRM1	+ 100	- 18.6	+ 16.0	- 15.6

Since for this scenario there is no significant difference between the X and the Y arm, tolerances are valid for both configurations.

6.4.2 Compensation of errors on ROCs.

Fig. 14 and 15 show the percentage variations of lprm2 needed to recover the stability of the NDRC in case of PRM3 and PRM2 ROCs manufacturing errors ; as for the previously described scenarios, variations of lprm2 length are determinant to restore the stable working point of the cavity.

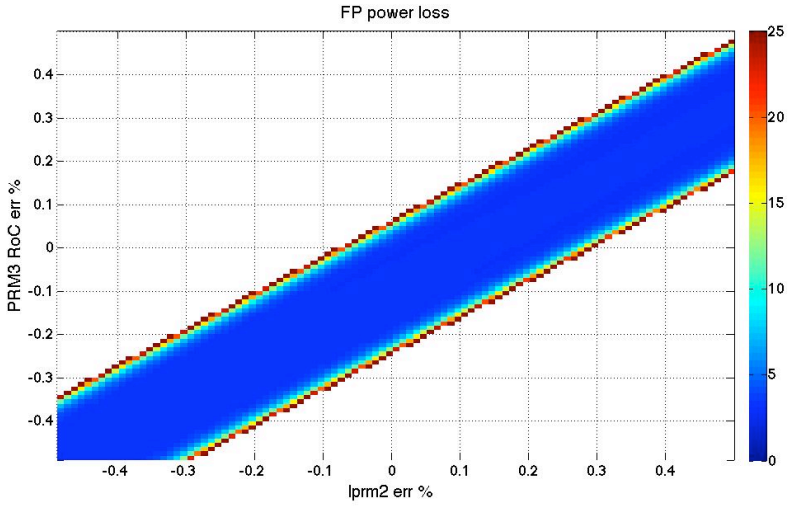

Figure 14 : Stability plot, PRM3 ROC manufacturing error VS lprm2, **design n.4**

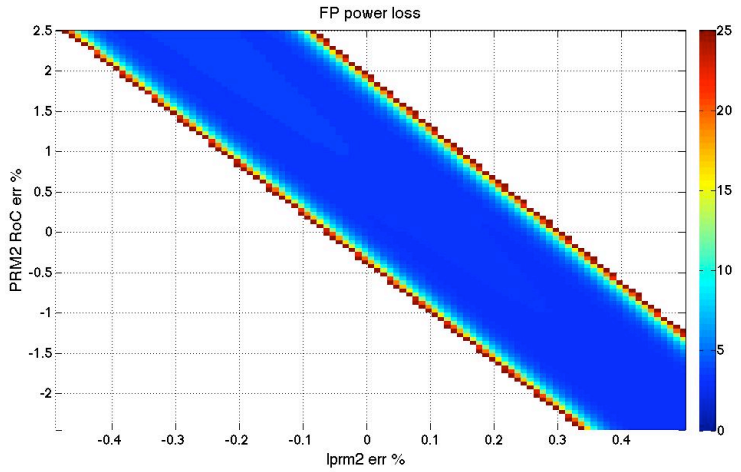

Figure 15 : Stability plot, PRM2 ROC manufacturing error VS lprm2, **design n.4**

6.5 Design n. 4bis.

6.5.1 Tolerances and losses.

The scenario 4bis is a modification of the scenario 4. The telescope is put in the differential part of the interferometer: PRM3 is suspended, together with the BS, at the BS superattenuator; PRM2 is suspended at the same super-attenuator of the ITM in the FP input tower, while RM1 is suspended in the power recycling tower.

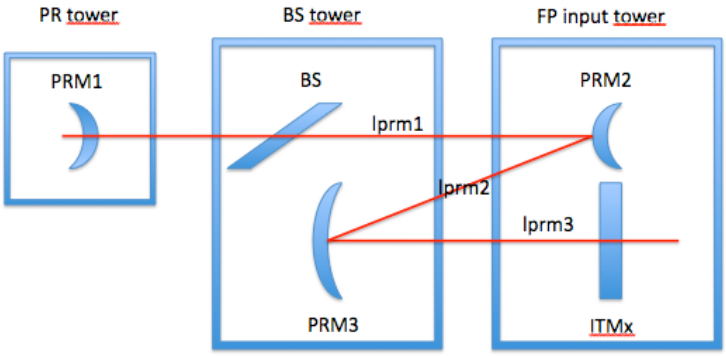

Figure 16 : rough optical scheme of scenario 4-bis

The calculated ROCs and the distances between optical elements are listed in the following tables, as well as beam parameter values in the NDRC. Beam parameter values refer to the sagittal propagation, for the beam *leaving* the optical element.

NDPRC option 4-bis	
Space	rough distance [m]
IMx - PRM3 (lprm3)	6
PRM3 - PRM2 (lprm2)	6
PRM2 – BS (lx)	6
BS - PRM1 (lprm1)	6

	IMX AR side	PRM3	PRM2	BS	PRM1
ROC [m]	Inf	- 13.6450	1.8503	Inf	3.7218
W [mm]	55.81	56.16	7.13	4.29	1.6
W0 [mm]	5.89	0.041	0.716	0.716	0.716
z [m]	976.94	- 6.87	- 15.14	- 9.20	3.7

The tilt angle is taken about 1.3 deg for both PRM2 and PRM3. With this values the single-trip Gouy phase in the NDRC is $\Phi_G = 21.7$ deg on the sagittal direction, $\Phi_G = 36.9$ deg on the sagittal direction, and astigmatism losses L_{FP} have the following values :

X arm 3.8 % Y arm 3.8 %

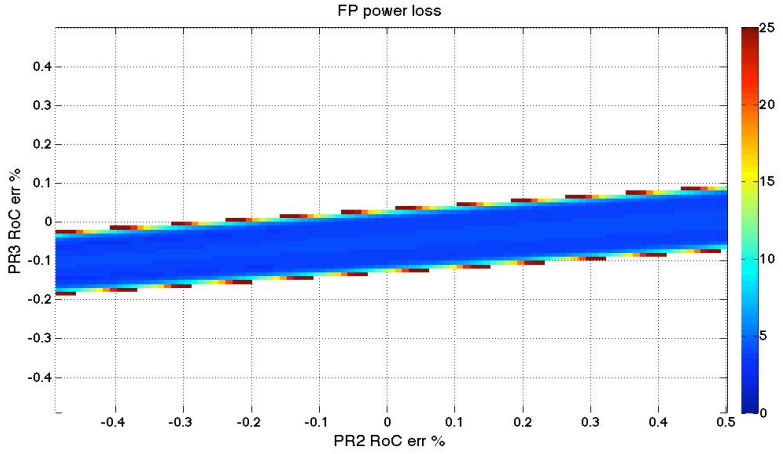

Figure 17 : Stability plot, **design 4-bis**

The tolerances for design 4-bis are :

	Stability tolerances %		Gouy tolerances % [10 deg < Φ_G < 30 (sagittal plane)]	
lx	+ 35.0	- 10.4	+ 7.6	- 8.0
l3	+ 100	- 100	+ 100	- 100
l2	+ 0.15	- 0.03	+ 0.027	- 0.026
l1	+ 20.0	- 10.5	+ 8.05	- 8.1
PRM3	+ 0.02	- 0.13	+ 0.02	- 0.03
PRM2	+ 1.15	- 0.20	+ 0.2	- 0.2
PRM1	+ 100	- 17.0	+ 20.0	- 13.6

Tolerances are valid for both configurations, because for this scenario there is no significant difference between the X and the Y arm.

Fig.18 and 19 show the variation of lprm2 needed to recover the stability of the NDRC in case of PRM3 and PRM2 manufacturing errors; as for the previously described scenarios, variations of lprm2 length are determinant to restore the stable working point of the cavity.

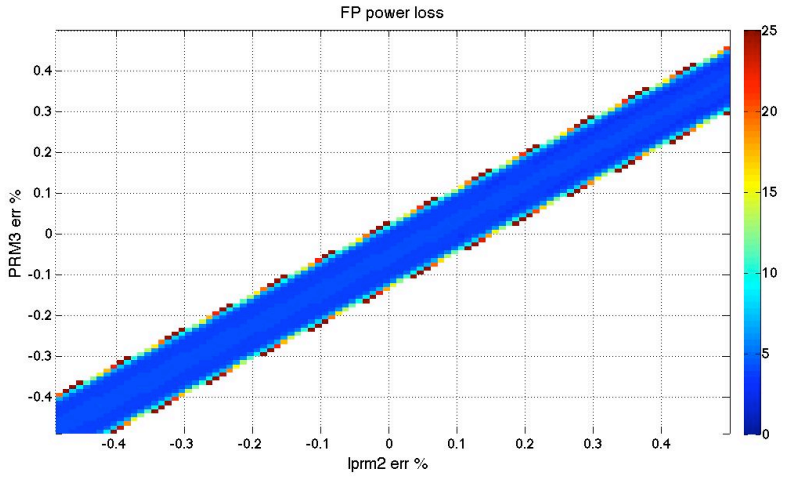

Figure 18 : Stability plot, PRM3 ROC manufacturing error VS lprm2, **design n.4-bis**

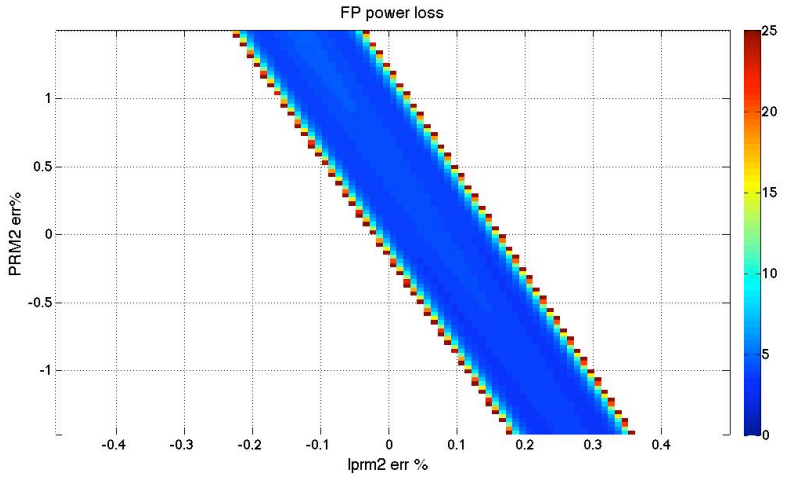

Figure 19 : Stability plot, PRM2 ROC manufacturing error VS lprm2, **scenario n.4-bis**

7. Thermal effects

Variations of the working point of the NDRC, leading to higher losses or instability, can be induced not only by manufacturer errors, but also by thermal effects.

The thermal effects in the NDRC can be even more important than the manufacturer errors, since they may be changing in time. The interferometer will be probably working in different thermal regimes: the lock acquisition will be possibly done in a *cold* state, with only a few Watts of input power, while the steady state corresponds to a *hot* state with a hundred Watts of input power.

In the following we present some simulations about the thermal effects in NDRCs, for the design n. 2 e 4 discussed previously ; these simulations have been run using the same Matlab based code which was used for astigmatism loss and stability tolerances estimations.

Under suggestion of TCS group, we have included in the simulations of NDRCs a thermal focal length f = 4.5 km, just after the ITM AR surface, to simulate the change in the optical

path length induced by absorption in ITM (we call this new configuration *hot interferometer*); then we run our simulations for stability and mismatch losses in the FP as described in the previous sections.

For each NDRC design simulated with hot interferometer configuration, stability plots are given.

7.1 Design n.2

The optical parameters of this design are those given in section 6.1 ; a thermal lens of f = 4.5 km is put just after the ITM AR surface. The results of the simulation are shown in figure 20:

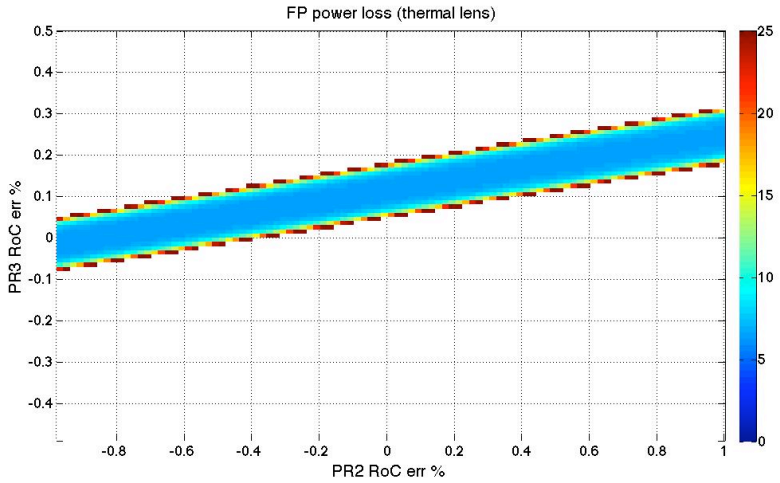

Figure 20 : Thermal effect stability plot, **design n. 2**

In fig.20 one can clearly see that the (0%, 0%) working point of the hot interferometer configuration is situated in the region of NDRC instability (white region), because only the sagittal direction is stable.

In other words, without the thermal compensation system the *hot* recycling cavity is not stable (or viceversa : if the recycling cavity is designed to be stable for the hot state, it will not be stable for the cold state).

If the focal lenght is the same for the two arms, it is possible to compensate for this instability, changing the ROCs of the telescopes (which in this configuration is in the common part of the interferometer).

To recover the stability region, a change of about + 0.1 % of PRM3 ROC (corresponding to a variation of PRM ROC of about 1 cm) is needed, or alternatively a decrease of PRM2 ROC of at least 0.5% (corresponding to a variation of about 2 cm) is needed. These changes in the telescope mirrors should be potentially achieved by the thermal compensation system ; otherwise, a change of lprm2 of the same amount of the needed change on PRM3 ROC could be realised, as shown in the section 6.2.2 of this note.

The simulated thermal effects do not change the overall mismatch losses of this design, and by changing PRM3 and PRM3 ROCs (or the distance lprm2 between them) the nominal Gouy phase value for this NDRC design can be achieved once again.

7.2 Design n.4

The optical parameters of this design are those given in section 6.5 ; a thermal lens of f = 4.5 km is put just after the ITM AR surface. The results of the simulation are shown in figure 21:

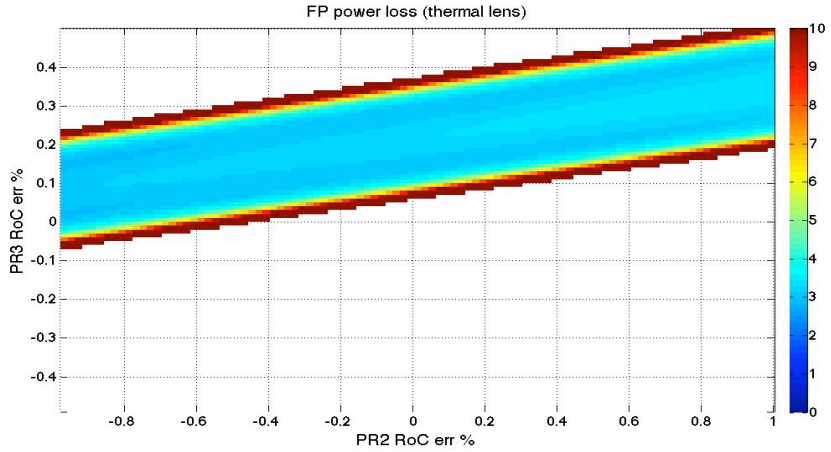

Figure 21 : Thermal effect stability plot, **design n. 4**

In this design the telescope is in the differential part of the interferometer (short Michelson). Then, the TCS can independently compensate for this effect acting on PRM3 and PRM2 ROCs. This design could allow to remove the compensation plates from the ITM reference masses.

Referring to fig. 15, for this design the hot interferometer NDRC working point (0% , 0%) is in the region of NDRC instability (white region of the plot) ; then, in order to recover the stability of NDRC, the TCS should be able to achieve a change of PRM3 ROC of the order of + 0.1 % (corresponding to a change of about 3 cm of the ROC) or a decrease of at least 1 % of PRM2 ROC (corresponding to a change of about 4 cm of the ROC).

The TCS group simulated [9] for this scenario a system of ring heaters, placed a few cm (about 2.5 cm) away from PRM3 and PRM2, for mirrors of 15 cm thick and a diameter of 35 cm (PRM3) and 20 cm (PRM2) ; in their simulation, the incident power on mirrors was 15 W. This compensation system can achieve a change of mirror ROCs of the order of 0.01 % for PRM3 and of 0.001 % for PRM2, not enough to compensate to the variations described above.

In order to increase the efficiency of the TCS, an optimization of the size and thickness of PRM2 and PRM3 should be investigated, togheter with the use of a CO2 laser instead of (or in parallel with) the heating ring.

We would like to remark that, in order to face the problem of stability of the cold and hot recycling cavity, the adLIGO team is considering the possibility to design the NDRCs for an intermediate value of the injected power in the interferometer [10].

8. Conclusions and comments

For each different design, the losses L_{FP} (measured with the overlap integral method) are :

Design # 1	Losses : 1.3 %
# 2	6.8 %
# 3	3.7 %
# 4	3.3 %
# 4 bis	3.8 %

The overall order of magnitude of the tolerances are the following :

ROCs

- PRM3 : 0.02 % to 0.04 % .
- PRM2 : 0.1 % to 0.3 % .
- PRM1 : 10 % .

This tolerances have to be compared with the manufacturer errors on ROC, and to the changes in ROCs due to the power absorbed by each mirrror.

Lengths :

- lprm3 : ± 100 % .
- lprm2 : 0.02 % to 0.05 % .
- lprm1 : 1 % to 8 % .

Except for design n.1, for all the proposed designs the most critical parameters -from a point of view of both NDRC stability and cumulated Gouy phase- are the ROCs of RM3 and RM2, and the distance lprm2 between these two mirrors. All the other parameters (lprm3, lrpm1, PRM1 ROC) can change of more than a percent without noticeably affecting the stability or the Gouy phase of the design n. 2, 3, 4, 4 bis.

For the design n.1, the tolerances on PRM3 and PRM2 ROCs are slightly more relaxed (of the order of 0.1 % for both mirrors), but those on the ITM AR lens are of the order of 0.01 % .

From the point of view of the coupling losses L, design 1 (L = 1.3%) and design 4 (L = 3.3%) seem to be the best candidates, but there are some problems that should be further studied. In the design 1 the backscattered light from ITM AR lens must be considered: to avoid this problem the lens can be tilted, and in this document a tilt of the lens of 1 deg has been simulated ; astigmatism losses could be higher and the NDRC stability could be decreased with a higher tilt of the lens. For the design 4 the potential sources of differential noise have not been considered at all.

From the point of view of the ROC/Gouy tolerances, all scenarios (except for scenario n.1)

have tolerances of the same order of magnitude for each mirror; in scenario n.1, the ITM AR lens ROC has a tolerance of the same order of magnitude of RM3 in the other designs (R3 is the most critical element in other designs).

The tolerance on the stability for thermal effects has been simulated only for design n.2 and n.4, but the results can be easily extended to the other designs ; from this point of view all scenarios -except n.1- are almost equivalent, i.e. their design is not stable at the same time for the 'cold' (low power) and 'hot' (full power) interferometer.

The impact of the astigmatism on the adVirgo sensitivity is a crucial point to be adressed. Moreover, the decrease of the astigmatism by optimization of the tilt angles (see for example [11]) and ROCs of RM2 and RM3 should also be explored.

Appendix A

Simulation of the coupled cavities : comparison between *Finesse* and the overlap integral

We have considered a double cavity system, where the first cavity is the advanced Virgo NDRC baseline power recycling cavity and the second one is the FP cavity of the interferometer arm (see figure A1 below).

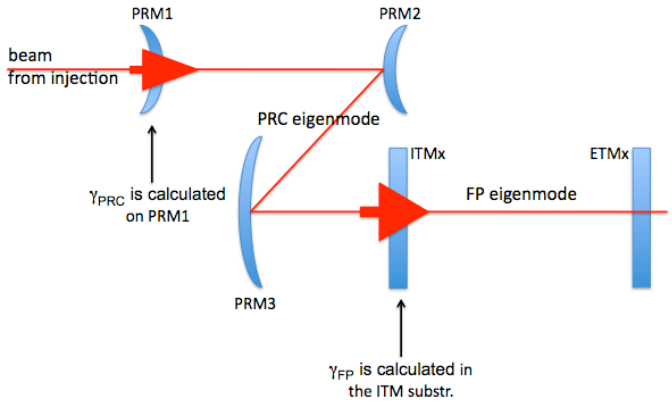

Figure A1 : Coupled cavity system

The angles of the power recycling mirror are for sake of simplicity artificially set to zero. Then the power recycling cavity is not astigmatic.

Two different simulations have been performed :

A.1 Mismatching between input beam and PRC, matched PRC and arm cavities.

The input beam has been changed from a perfect matching, while the matching between the two cavities is perfect.

- The overlap integral (OI) matching losses are: $L_{coupling} = 1 - \gamma^2_{PRC}$.
- The losses measured with *Finesse* are $L_{Fin} = 1 - P/P_0$, where P and P_0 are the power stored in the arm cavity respectively with and without mismatching.

Results of this first simulation are shown in fig.A2 ; *Finesse* was run with high order modes (HOMs) modal expansion, and no 'cav' command [12] was set on cavities (modal expansion only). A good agreement between OI and *Finesse* results was found.

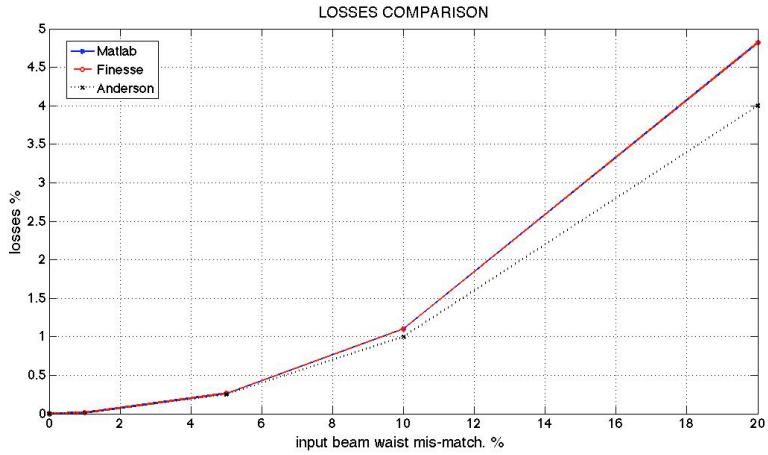

Figure A2 : Coupled cavity scenario, input beam mismatch losses.

A.2 Input beam perfectly matched with PRC, mismatching between PRC and FP arm cavity.

In order to change the matching between the two cavities we change the ROC of PRM1. For each PRM1 value we adjust the input beam to be perfectly matched with the mode of the PRC cavity. Only the two FP and PRC cavities are mismatched.

Results reported in fig.A3 show a strong disagreement between OI and *Finesse* results, with *Finesse* losses much higher than OI ones ; also in this case *Finesse* has been run with HOMs modal expansion and no 'cav' command [12] set on cavities.

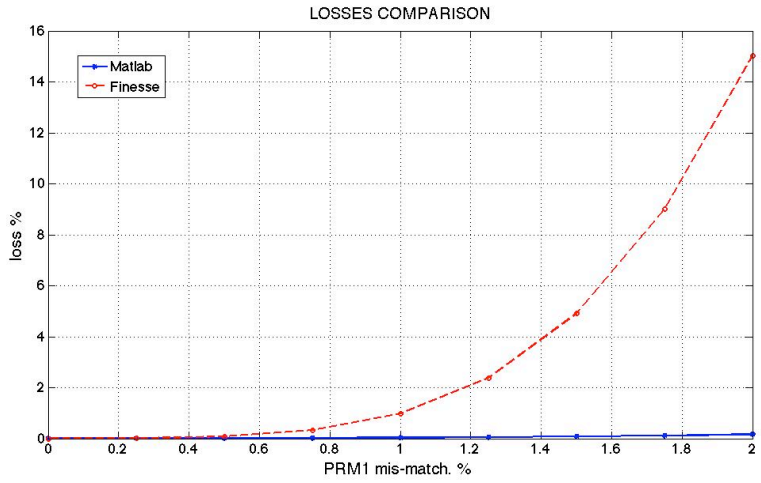

Figure A3: Coupled cavity scenario, cavity mismatch losses.

This disagreement is probably due to the insufficient number of modes (10) used in the simulation.

It could be eliminated by using the command 'cav' [12], which takes in account the eigenmodes of the two cavities, instead making an espansions in modes, and using the 'phase 2' command [12] for the computation of *Finesse* reflectivity/transmissivity coupling

coefficients (for the details see [12], sections 4.5 to 4.8 included, and also the general definition given in [13]).

Because of some persistent computing problems about reflectivity/transmissivity coupling coefficients on the AR side of the ITM of the FP, the ITM has been subsequently treated in the new *Finesse* simulation as a mirror with no thickness.

The results of this new *Finesse* simulation are shown in fig.A4, where OI estimations and *Finesse* and OI results are compatible whithin of the order of 10%, for mismatching losses up to 2 % .

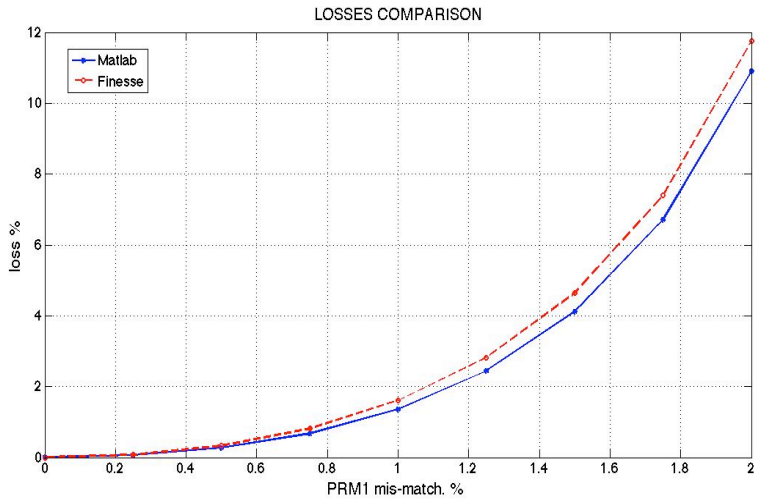

Figure A4 : Coupled cavity scenario, cavity mismatch losses, new Finesse settings, no thick lens in ITM.

Using different sets of eigenmodes for the resonating cavities, A. Freise showed [14] in a parallel simulation that the *Finesse* coupling losses could be much lower than the ones shown in fig.4 ; since up to now there is no clear indication about the best choice of the eigenmode sets to be used, this issue must be further investigated.

A.3. Comments and conclusions.

Using 'cav' and 'phase2' commands [12], *Finesse* and the OI Matlab based code agree for the coupled cavity system, with the advaced Virgo parameters (no astigmatism) and with a particular choice of the eigemode sets of the resonating cavities.

In the case of coupled cavities, OI results were also confirmed by M. Arain and H. Yamamoto [6] with indipendent simulations (FFT code).

References

[1] Freise A. et al. , *Advanced Virgo design: Layout options for the non-degenerate Recycling Cavities*, Virgo internal note VIR-025A-09.
[2] Arain M. A. , Mueller G. , *Design of the Advanced LIGO Recycling Cavities*, Opt. Expr., vol. 16, issue 14, 2008.

[3] Virgo coll. , *Advanced Virgo Baseline Design*, Virgo internal note VIR-027A-09.
[4] http://www.rzg.mpg.de/~adf/
[5] Anderson D. Z. , *Alignment of Resonant Optical Cavities*, Appl. Opt. vol. 23, n. 17, 1984.
[6] Arain M. A. , private communication.
[7] Massey G. A. , Siegman A. E. , *Reflection and Refraction of Gaussian Light Beams at Tilted Ellipsoidal Surfaces*, Appl. Opt. vol. 8, n. 5, 1969.
[8] Arain M. A. , *Analysis of Mode Mismatch due to Astigmatism at Recycling cavity Mirrors*, LIGO internal note T080315-00-Z.
[9] Fafone V. , Rocchi A. , Advanced Virgo Biweekly Meeting, 12/03/2009.
[10] Mueller G. , Arain M. A. , private communication.
[11] Hello P. , Man N. , Virgo internal note VIR-NOT-LAS-1390-012
[12] Freise A. , FINESSE 0.99.6 Manual, 28/02/2008 release.
[13] Bayer-Helms F. , Appl. Opt. vol. 23, n. 9, 1984.
[14] Freise A. , private communication.